Theoretical study of multielectron dissociative ionization of diatomic molecules and clusters in a strong laser field

Isidore Last and Joshua Jortner
School of Chemistry, Tel-Aviv University, Tel Aviv 69978, Israel
(Received 22 January 1998)

The analysis of electron potentials in multicharged molecules and small clusters allows one to determine which of these systems may be ionized in a strong laser field by the quasiresonance mechanism. The presence of moderately transparent interionic potential barriers (for electron tunneling) is necessary for the quasiresonance electron energy enhancement and, consequently, for ionization [Zuo and Bandrauk, Phys. Rev. A **52**, R2511 (1995)]. In multicharged systems, which spatially expand by Coulomb explosion, the interionic barriers increase with time. The simulation of electron motion in such systems demonstrates the presence of a different kind of charge resonance enhanced ionization mechanism whose efficiency depends on the dynamics of the increase of the interionic barriers. This dynamic charge resonance enhanced ionization mechanism is of classical origin and its efficiency is higher than that of the static (frozen geometry) mechanism.
[S1050-2947(98)06410-5]

PACS number(s): 33.80.Rv

I. INTRODUCTION

The effect of ionization on the stability of molecules and clusters strongly depends on the ionic charge. When a system loses only a single electron then the interaction energies between the ionized atom and the surrounding atoms are changed by not more than several eV. In single charged van der Waals (vdW) clusters an excess energy of about 1 eV is released due to the formation of a valence bound ionic core. This excess energy usually causes evaporation of neutral atoms, which decreases the cluster size [1–3]. The situation is different in doubly charged systems where the charge is located on two different ions, so that the Coulomb repulsion becomes the main cause of instability [4–6]. In molecules and in small and intermediate size clusters the Coulomb repulsion induces Coulomb explosion. The Coulomb explosion of clusters is realized as a fission into two singly charged clusters [7–11]. The time scale of the Coulomb explosion of such vdW clusters is of the order of several (or tens of) ps [12], whereas in valence clusters this process can be longer by several orders of magnitude [9]. The Coulomb explosion process of triply charged clusters is similar to that of doubly charged clusters, with the obvious difference in the number of the product of singly charged clusters [13,14]. The doubly and triply charged clusters, as well as some ionic clusters with larger charge, e.g., C_{60}^{7+} [15], are produced by the usual techniques of electron impact or x-ray ionization.

Much higher levels of multielectron ionization can be achieved by photoionization in a strong laser field [16–28]. Multielectron ionization of diatomic molecules in a strong laser field leads to Coulomb explosion and to the production of atomic ions, as in the case of doubly ionized molecules, with the difference in the product ions charge [18–21]. Such a process of the atomic ion production is called multielectron dissociative ionization (MEDI). The kinetic energy of atomic ions produced by MEDI increases with increasing ion charge. For example, the kinetic energies of the N^{2+} and N^{3+} ions, which are the products of the N_2^{4+} and N_2^{6+} dissociation, are 5–15 and 15–25 eV, respectively [18]. In clusters the multielectron ionization in a strong laser field usually leads to the ionization of all cluster atoms and consequently to a very strong Coulomb explosion whose products are atomic ions [23–28]. The kinetic energy of these product ions is much higher than in diatomic molecules due to the large number of interacting charged particles. Thus MEDI of small $HIAr_n$ ($n \leqslant 8$) clusters produces Ar^{3+} ions with a kinetic energy of 204 eV [23], which is about one order of magnitude higher than the kinetic energy of the N^{3+} ion produced by the MEDI of a highly charged ($+4$ or $+6$) nitrogen molecule. The kinetic energy of the MEDI product ions is expected to increase with the cluster size [29]. When large clusters, containing 1000 or more atoms, are subjected to the MEDI process, the kinetic energy of multicharged product ions is in the range of hundreds of keV or even about 1 MeV [26–28].

Since the multielectron ionization of molecules or clusters in a strong laser field involves tens or even hundreds of photons, the quantum nature of the light absorption is practically lost and a classical treatment of the light field becomes appropriate [30]. Accordingly, one may try to treat the ionization in a strong laser field in the same way as in an electrostatic field, at least in the case where the light frequency is considerably lower than the characteristic frequency of electron motion. In an electrostatic field, bound states are separated from the unbound (ionized) states by an electrostatic barrier. In a neutral atom subjected to a relatively weak field the excited electrons can tunnel over this electrostatic barrier [31]. However, in the case of ground-state multicharged atomic ions the electrostatic mechanism is of minor importance since the barrier is high and wide and the tunneling probability is negligibly small. Only in extremely strong fields, when the outer field is comparable with the atomic one, the electrostatic barrier disappears and the ground-state ionization can be realized by direct electron removal. In a single charged ion such a kind of ionization is characterized by an outer field F with the force eF of a few eV/Å, but in order to remove an electron from a multicharged atomic ion one needs an outer field of tens or hundreds of eV/Å.

 ©1998 The American Physical Society

In a multicharged polyatomic system ions can be deprived of some of their electrons not only by the outer field but also by the inner Coulomb field, giving rise to ionization via the ignition model [25,32]. The electrons removed from the ions are usually kept inside the multicharged polyatomic system because of its large total positive charge. These electrons can be removed from the system only in the case when their energy is significantly enhanced. It follows that in order to explain the subsequent ionization steps in the already charged polyatomic system one needs to find a mechanism of electron energy enhancement.

Some of the features of MEDI of diatomic molecules are explained, at least qualitatively, by a model of molecule stabilization in a strong laser field [33]. Such stabilization is known to be expected in neutral molecules due to a coupling between the ground state and an excited molecular state that is in resonance with the laser field [34]. The potential well for this stabilization in strong fields is of the order of a few eV. In multicharged molecules, however, the stabilization effect is most probably weaker due to a weaker coupling between molecular states. At the same time the Coulomb repulsive potential between, for example, fourfold ionized ions is of the order of 50–100 eV. Such strong repulsion makes the stabilization mechanism doubtful, except, possibly, for the case of singly charged molecules [35].

A description of the MEDI in diatomic molecules rests on models that take into account that the electron motion between two ions can be slowed down by an inner potential barrier [36–39]. This barrier rises with the interionic distance so that at some distances the characteristic frequency of the electron motion becomes close to the light frequency, providing a quasiresonance enhancement of the electron energy. Such a mechanism of the electron energy enhancement was first proposed by Zuo, Chelkowski, and Bandrauk for the simplest ionic molecule H_2^+ [36]. When the electron energy enhancement results in ionization the process is referred to as a charge resonance enhanced ionization (CREI) [37,38]. The quantitative treatment of the MEDI process in multicharged diatomic molecules was recently advanced by Seideman *et al.* [39] and by Chelkowski and Bandrauk [38]. Both treatments [38,39] rest on the frozen nuclear geometry approximation. The aim of the present work is dual. First, we will consider the effect of the electron potential features on the CREI process, attempting to predict which molecules and vdW clusters are expected to be subjected to MEDI by the CREI mechanism. Second, we will treat the CREI process in Coulomb exploding multicharged systems, discarding the frozen geometry approximation [40]. We advance a different kind of CREI mechanism in these systems that will be referred to as dynamic CREI. The dynamic CREI mechanism is of classical origin and its efficiency is mostly higher than the efficiency of the static frozen geometry models [38,39].

The CREI mechanism in diatomics will be described in the next section. The CREI of vdW clusters will be treated in Sec. III. In Sec. IV we will present the dynamic CREI process in Coulomb expanding systems. The final results of this study will be summarized in Sec. V.

II. THE CREI MECHANISM IN DIATOMIC MOLECULES

Let us consider a diatomic molecule oriented along the outer field. In the presence of an outer static field F the

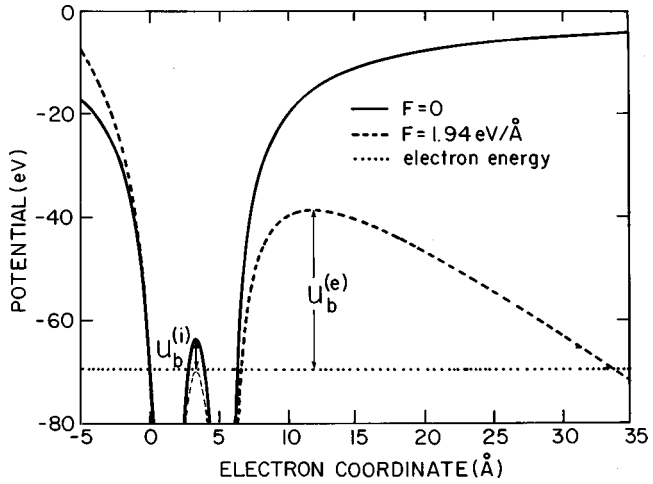

FIG. 1. Electron potential in the absence of an outer field ($F=0$) and in the field $eF=1.94$ eV/Å for $I^{5+}Ar^{4+}+e$ with $R_{IAr}=4.06$ Å.

electron can go to infinity by overcoming the electrostatic barrier $U_b^{(e)}$ (Fig. 1). The height of this barrier depends on the initial location x_0 of the electron, as the one-dimensional potential (to be utilized herein) in the presence of the outer field is

$$V_F(x)=V(x)-eF(x-x_0), \tag{1}$$

where $V(x)$ is the inner potential of the electron interaction with ionic cores. If the electron can move freely inside the molecule, then the longest electron free path l and, consequently, the lowest electrostatic barrier will be provided by an electron located initially at the molecule end that is opposite to the field direction (at $x_0=0$ in Fig. 1). In this case l exceeds the interatomic distance, whereas in atoms l is of the order of the electron orbit diameter. Due to a longer free path of electron motion, molecules can exhibit lower electrostatic barriers than atoms [41]. However, in moderately strong laser fields the electrostatic barrier in multicharged molecules is still not sufficiently low to make the ionization feasible. Much more efficient is the CREI mechanism, which takes into account the alternating character of the laser field [37,38]. When the characteristic frequency of the electron motion ν_e between ions is of the order of the light frequency ν_F, a quasiresonance process can lead to the enhancement of the electron energy up to the level that allows the electron to overcome the electrostatic barrier and to leave the molecule. The quasiresonance condition is not satisfied at small interionic distances when an electron is moving freely inside a molecule, since the characteristic frequency ν_e of a freely moving electron is much higher than the light frequency ($\nu_e \gg \nu_F$). When the interionic distance R increases, the electron potential in the region between the ions becomes higher and at some interionic distance R_b a barrier appears that can be overcome by tunneling only. This inner barrier decreases the electron motion frequency ν_e so that at some distance $\sim R_{rs}$, when $\nu_e \sim \nu_F$, the quasiresonance conditions are met and the efficiency of ionization drastically increases. At interionic distances R that are larger than R_{rs} the barrier transparency becomes very low, preventing any enhancement of the electron energy. Consequently, the ionization efficiency

TABLE I. The distances (in angstroms) of zero barrier R_b and nontransparent barrier R_T (see text) for $Cl^{q+}Cl^{q+}$ at different laser fields. In the presence of an outer field only R_T values are shown. For the outer field both laser power S and field strength $eF=eF_0/\sqrt{2}$ are presented. Dashes indicate where R_T has not been found ($R_T>10$ Å). The atomic IP are also presented in the table.

S (W/cm^2)	eF (eV/Å)	q / IP (eV)	1 12.97	2 23.81	3 39.61	4 53.47	5 67.80	6 97.03
0	0	R_b	3.32	3.62	3.27	3.23	3.18	2.68
		R_T	4.46	4.46	3.93	3.80	3.69	3.04
10^{13}	0.614	R_T	5.26	4.88	4.10	3.92	3.78	3.13
10^{14}	1.94	R_T	—	6.6[a]	4.62	4.25	4.41	3.24
10^{15}	6.14	R_T	—	—	—	6.9[a]	5.3[a]	3.67

[a]There is no electrostatic barrier.

dependence on the interionic distance R exhibits a (usually wide) maximum around the interionic distance R_{rs}. Such behavior of the ionization efficiency was well demonstrated [38,39], with the ionization process being characterized by one-dimensional wave-packet propagation for frozen molecule geometry.

The CREI process cannot be realized if the quasiresonance conditions are met at interionic distances R_{rs} smaller than the equilibrium distance R_e of the neutral molecule. In the case where $R_{rs}>R_e$ the neutral molecule may become singly or doubly ionized in the beginning of irradiation ($R=R_e$) due to the electrostatic barrier suppression and a direct electron removal. After such initial ionization takes place, the distance R between ions begins to increase. When R approaches the interval of the quasiresonance energy enhancement, more electrons are removed and the molecule becomes multicharged [38,39]. Due to the CREI mechanism, molecules exhibit a higher efficiency of multielectron ionization than atoms.

Because of the importance of the inner potential barrier for CREI, let us consider the electron potential U in a multicharged diatomic molecule. In the absence of the outer field the potential U is determined by electron interaction with two ions. We will describe this interaction by the Coulomb potential ignoring the potential behavior inside the ion cores. Such a presentation of the electron potential is usually well justified in the middle of a multicharged molecule where the inner barrier is located.

In the case of the ionization process in a homonuclear molecule

$$A_{(1)}^{(q-1)+}A_{(2)}^{q+}\rightarrow A_{(1)}^{q+}A_{(2)}^{q+}+e \tag{2}$$

the Coulomb potential $V(x)$ along the molecular axis x [with $V(\infty)=0$ and with $x=0$ taken at the molecule center] is

$$V(x)=-4BqR/(R^2-4x^2), \quad B=14.385 \text{ eV/Å}. \tag{3}$$

In the Coulomb potential approximation the ionization potential (IP) of the multicharged molecule is

$$I^{(q)}=I_0^{(q)}+Bq/R, \tag{4}$$

where $I_0^{(q)}$ stands for the atomic IP of the ion $A_{(1)}^{(q-1)+}$. The potential (3) has a maximum at $x=0$ that will be called an inner maximum

$$V_\sharp^{(i)}=-4Bq/R. \tag{5}$$

When the electron energy $-I^{(q)}$ is lower than $V_\sharp^{(i)}$, the potential (3) forms a barrier that separates the two potential wells of the ionic molecule $A_{(1)}^{q+}A_{(2)}^{q+}$. The height of this inner barrier $U_b^{(i)}$ and its width $d_b^{(i)}$ at the electron energy $-I^{(q)}$ are

$$U_b^{(i)}=V_\sharp^{(i)}+I^{(q)}=-3Bq/R+I_0^{(q)} \tag{6}$$

and

$$d_b^{(i)}=R(U_b^{(i)}/I^{(q)})^{1/2}; \quad U_b^{(i)}>0. \tag{7}$$

The inner barrier ($U_b^{(i)}>0$) exists at interionic distances $R>4Bq/I^{(q)}$. At these distances the electron is classically localized on one of the ions and only the quantum effect of tunneling can lead to electron motion between the ions. Taking into account the IP dependence on R, Eq. (4), one obtains a simple expression for the distance R_b of the barrier emergence ($U_b^{(i)}=0$) [38,39]

$$R_b=3Bq/I_0^{(q)}. \tag{8}$$

Equation (8) refers to the absence of the outer field. As shown in Ref. [38], the presence of an optimal outer field modifies this R_b to $\sim 4Bq/I_0^{(q)}$.

The simple expression (8) rests on the Coulomb potential approximation, which is well satisfied in multicharged molecules. It is also important to note that this expression includes one atomic parameter only, i.e., $I_0^{(q)}$. The distance R_b indicates the onset of the sharp decrease of the electron motion frequency ν_e, which leads to the quasiresonance condition $\nu_e\sim\nu_F$. The ionization is precluded at distances where the barrier is nontransparent. Denoting by R_T the distance where the inner barrier becomes nontransparent, one can put the distance R_{rs} of a high ionization efficiency inside the limits $R_b<R_{rs}<R_T$. As the measure of the barrier transparency we will use the parameter T, which determines the tunneling probability through a square barrier as proportional to $\exp(-T)$ [42]. When the barrier is not exactly of the square shape, as in our case (Fig. 1), the parameter T can be expressed by an integral

$$T=1.024\int dx[V_F(x)+I^{(q)}]^{1/2}; \quad V_F(x)+I^{(q)}>0. \tag{9}$$

In Eq. (9) the energy values are in eV and the distance is in Å. In the case of Coulomb potential ($F=0$) the integral (9) is well fitted by an analytical expression

$$T=0.82R[I_0^{(q)}-3Bq/R][I_0^{(q)}+Bq/R]^{-1/2}. \quad (10)$$

The tunneling probability is close to 1 for $T\ll 1$ and small for $T>1$. We suggest considering a barrier to be of low transparency when $T>3$, i.e., $\exp(-T)<0.05$.

The R_b distance is presented in Table I for the multicharged Cl_2 molecule. In the range $1\leqslant q\leqslant 5$ the distance R_b depends weakly on q due to the almost linear $I_0^{(q)}$ dependence on q for the ionization of p electrons. When the first s electron is removed ($q=6$) the distance R_b decreases significantly. But for all q values presented in Table I, R_b values are larger than the equilibrium interatomic distance $R_e=1.998$ Å of a neutral molecule. In other valence bound molecules, at least for outer-shell electrons, the condition $R_b>R_e$ is fulfilled as well. For example, in the I_2 molecule R_b is about 4 Å, being a much larger value than the equilibrium distance $R_e=2.667$ Å. Due to the absence of inner barriers at initial (equilibrium) distances R_e valence molecules are expected to exhibit the CREI mechanism, in accordance with the original conclusions [38,39].

We will now take into account the outer field F effect on the electron potential $V_F(x)$, Eq. (1). In order to get the strongest effect on the potential we will put the initial electron position at the classically available extreme left point, determined as $V(x_0)=-I^{(q)}$ ($x_0=0$ in Fig. 1). As the field strength we will take a value F to be smaller than the field amplitude F_0, namely, $F=F_0/\sqrt{2}$. The field amplitude is connected with the average energy flux S by the equation

$$eF_0=2.745\times 10^{-7}S^{1/2}. \quad (11)$$

where S is expressed in W/cm^2 and eF_0 in eV/Å. The laser field dependence of the R_T distances of Cl_2 is presented in Table I. In the case of $q=3$ and $S=10^{14}$ W/cm^2 we have $R_b=3.3$ Å and $R_T=4.6$ Å, whereas Ref. [38] provides ionization efficiency maxima at $R=3.8$–5.0 Å. This example confirms that the R_b and R_T distances may provide useful information about the location of the high efficiency ionization region. In the case of a very strong field of $S=10^{15}$ W/cm^2 the potential is so strongly depressed, at least for $q<4$, that at small interionic distances both inner and electrostatic barriers are absent and electrons can be removed directly by the field, without any quasiresonance energy enhancement. Consequently the ionization is expected to take place at $R\sim R_e$ (vertical ionization), as supported experimentally [18].

In contrast to the valence molecules, the vdW rare-gas and rare-gas–halogen diatomic molecules have inner barriers at equilibrium distances R_e in any charged state. This feature of these vdW diatomics originates from much larger equilibrium distances R_e but is not due to smaller zero barrier distances R_b. The transparency parameters T of the inner barriers of Ar_2, Xe_2, and IAr diatomics at the equilibrium geometry are presented in Table II for the ionization process of the q-charged ion production:

$$A_{(1)}^{(q-1)+}A_{(2)}^{(q-1)+}\rightarrow A_{(1)}^{q+}A_{(2)}^{(q-1)+}+e, \quad (12)$$

TABLE II. Tunneling parameters T for vdW diatomics ArAr, XeXe, and IAr at equilibrium geometry ($R_e=3.76$, 4.37, 4.06 Å, respectively) for different outer fields eF (in eV/Å). The ionization process is shown by Eq. (12). The atomic IP (in eV) are also presented in the table. The absence of both inner and electrostatic barriers is denoted by ellipses. The absence of an inner barrier in the presence of an electrostatic barrier is denoted by no entry.

eF \ q	2	3	4	5	6	7
			ArAr			
IP	27.6	40.7	59.8	75.0	91.0	124
0	5.08	4.70	6.67	7.12	7.78	12.5
1.94	1.90	2.20	4.74	5.43	6.27	11.3
6.14	⋯	⋯	0.25	1.54	2.84	8.60
			XeXe			
IP	21.2	32.1	46.7	59.7	71.8	92.1
0	3.84	3.51	5.13	5.83	5.87	9.08
1.94	⋯			3.16	3.45	7.06
6.14	⋯	⋯	⋯	⋯		2.46
			IAr			
IP	19.1	33.0	44.0	55.3	75.8	87.5
0	1.39	2.62	2.36	2.34	5.42	5.37
1.94	⋯				3.38	3.49
6.14	⋯	⋯	⋯	⋯		

where the numbers in parentheses stand for atomic indexes. According to the results in Table II, in the absence of the outer field ($F=0$) the inner barriers of pure rare-gas diatomics are not transparent ($T>3$) preventing any electron motion between the ions. The inner barriers of Ar_2 are mostly nontransparent also in a relatively moderate field of $eF=1.94$ eV/Å ($S\sim 10^{14}$ W/cm^2), and only in a very strong field of $eF=6.14$ eV/Å ($S\sim 10^{15}$ W/cm^2) the inner barriers are significantly suppressed. Because of the presence of the inner barriers the multielectron ionization of Ar_2, at least by the CREI mechanism, is probably impossible. The situation is more favorable for the CREI mechanism in Xe_2 and IAr (for the electron potential in IAr see Fig. 1). However, even in the case of a relatively transparent inner barrier at R_e, the possibility of multielectron ionization looks doubtful, at least for larger values of q, since after a molecule becomes initially ionized at R_e the interionic distance begins to increase, which leads to the increase of the inner barrier, which prevents the electron motion between ions. In very strong fields the molecules are probably ionized by direct electron removal as in these fields both the inner and the electrostatic barriers are suppressed (Table II).

III. ELECTRON POTENTIAL IN MULTICHARGED vdW CLUSTERS

One distinction between the multicharged clusters and diatomic molecules is quite obvious, being due to the difference in the number of ions and, consequently, in the total charge of the system. Because of their larger total charge the IPs are higher in the charged clusters than in diatomics. In a multicharged cluster the IP of an ion (denoted by index i) is equal to the atomic IP $I_0^{(q)}$ minus the potential V_i generated by the other ions:

$$I_i^{(q)}=I_0^{(q)}-V_i;\quad V_i<0. \tag{13}$$

In the charge point approximation and in the case of uniformly charged cluster the potential V_i is

$$V_i=-Bq\sum_{j\neq i}\frac{1}{R_{ij}}. \tag{14}$$

Let us consider now a symmetrical and uniformly charged cluster in the presence of the outer field. The external (outside the cluster) electron potential is

$$V_F(x)=-\frac{Bqn}{x}-eF(x-x_0), \tag{15}$$

where n is the number of atoms, x is the distance from the cluster center, and x_0 is the initial location of the electron. When the electron is initially located at the cluster center ($x_0=0$) the maximum of the potential (15) is

$$V_\ddagger^{(e)}=-2(Bqn|eF|)^{1/2}. \tag{16}$$

It is located at

$$R_b^{(e)}=(Bqn/|eF|)^{1/2}. \tag{17}$$

Using Eqs. (13), (14), and (16) one obtains the electrostatic barrier for the ith ion ionization

$$(U_b^{(e)})_i=V_\ddagger^{(e)}+I_i^{(q)}=I_0^{(q)}+Bq\sum_{j\neq i}\frac{1}{R_{ij}}-2(Bqn|eF|)^{1/2}. \tag{18}$$

For realistic fields and for $q>2$ the electrostatic barrier, Eq. (18), usually increases with the cluster size and exceeds the electrostatic barrier of diatomic molecules.

Another distinction between multicharged clusters and diatomic molecules originates from the effect of the surrounding ions on the electron potential $V(x)$. This effect will be considered here for both adjacent and for nonadjacent pairs in small rare-gas clusters $\mathcal{R}_n$. Let us first consider two uniformly charged rare-gas clusters $(\mathcal{R}^{q+})_5$ and $(\mathcal{R}^{q+})_6$ in the geometry of the neutral clusters. It is important to note that because of a weak, $1/r$, dependence of the Coulomb potential on the electron-ion distance, the electron potential is not very sensitive to the system geometry. In the $(\mathcal{R}^{q+})_5$ cluster there is one pair of nonadjacent atoms (indexes $i=1,2$) separated by a distance $R_{12}=1.633R$, R being the interatomic distance between adjacent atoms. The electron potential along the x axis connecting atoms 1 and 2 ($x=0$ as the cluster center) is

$$V(x)=-Bq[2\sqrt{6}R/(2R^2-3x^2)+3\sqrt{3}/(R^2+3x^2)^{1/2}]. \tag{19}$$

In contrast to the electron potential in a diatomic molecule, Eq. (3), which reveals a maximum at $x=0$, the potential (19) exhibits a minimum at $x=0$ and two maxima at $x=\pm 0.2R$. In the $(\mathcal{R}^{q+})_6$ cluster there are three pairs of nonadjacent atoms with the interatomic distance $\sqrt{2}R$. The electron potential along a line connecting a pair of nonadjacent atoms in $(\mathcal{R}^{q+})_6$ is

TABLE III. Ionization potentials $I^{(q)}$ (in eV) and inner barriers U_b (in eV) in vdW clusters at equilibrium configurations. The interionic distances R_{12} are given in Å. The ionization process is shown by Eq. (21).

R_{12}	q	2	3	5	7
			Ar_5		
6.07	$I^{(q)}$	41.6	68.7	130.9	208.1
	U_b	+9.5	+7.8	+12.5	+32.2
			Ar_6		
5.26	$I^{(q)}$	45.8	77.1	147.8	233.5
	U_b	+8.7	+7.0	+11.9	+31.9
			Ar_{13}		
3.72	$I^{(q)}$	63.3	112.1	217.7	338.3
	U_b	+1.1	−4.6	−7.2	+4.4
			Xe_6		
6.08	$I^{(q)}$	37.0	63.6	122.7	186.6
	U_b	+4.8	+2.9	+5.1	+12.2
			IAr_3		
4.06	$I^{(q)}$	29.8	54.3	97.8	156.1
	U_b	+0.4	+1.8	−0.5	+12.1
			IAr_4		
4.06	$I^{(q)}$	32.0	58.7	106.7	169.3
	U_b	−0.4	+0.2	−3.4	+7.6
6.48	U_b	+0.5	−1.3	−10.2	−4.5
			IAr_5		
4.06	$I^{(q)}$	35.8	66.4	122.0	192.4
	U_b	−0.2	+0.6	−3.0	+8.3
5.72	U_b	−0.3	−2.1	−9.8	−2.1

$$V(x)=-4B[R/(R^2-4x^2)+2/(R^2+4x^2)^{1/2}]. \tag{20}$$

The potential (20) has a flat maximum around $x=0$, where both the first and the second derivatives are zero. The potential at the center is $V_\ddagger^{(i)}=-12Bq/R$. Due to the effect of surrounding ions the maxima of potentials (19) and (20) are much lower than in a diatomic molecule (where $V_\ddagger^{(i)}=-4Bq/R$). In larger clusters $(\mathcal{R}^{+q})_n$, $n>6$, the potential between nonadjacent ions demonstrates mostly two low maxima, as in the $(\mathcal{R}^{q+})_5$ cluster.

The important parameter of the CREI mechanism is the inner potential barrier $U_b^{(i)}$ [see Eq. (6)]. Since surrounding ions decrease $V_\ddagger^{(i)}$ but increase $I^{(q)}$, their effect on the potential barrier should be numerically analyzed. The potential barriers for some pure argon and xenon clusters and argon clusters with one iodine atom are presented in Table III. The multicharged clusters under consideration are taken in the geometry of neutral rare-gas clusters. The accepted interatomic distances between adjacent atoms are as follows: $R_{\text{Ar-Ar}}=3.72$ Å, $R_{\text{Xe-Xe}}=4.3$ Å, $R_{\text{I-Ar}}=4.06$ Å. Table III presents the ionization potentials and inner barriers for the ionization process

$$A_{(1)}^{(q-1)+}A_{(2)}^{(q-1)+}(A_{(k)}^{(q-1)+})_m \rightarrow A_{(1)}^{q+}A_{(2)}^{(q-1)+}(A_{(k)}^{(q-1)+})_m+e,\quad k=3,\ldots,n, \tag{21}$$

where (1), (2), and (k) stand for atomic indexes. The atomic $I_0^{(q)}$ IP data were taken from Ref. [43].

According to the results of Table III the small Ar_n clusters, $n \leqslant 6$, demonstrate relatively big inner barriers between nonadjacent ions. The inner barriers between adjacent ions (not shown in the Table III) are even bigger. These barriers are completely nontransparent and presumably prevent the ionization of small Ar_n clusters. If we take, for example, a not so big barrier of 7.0 eV (Ar_6, $q=2$), its tunneling parameter is as large as $T=6.4$. The presence of nontransparent barriers at equilibrium configuration can explain why Castleman *et al.* did not observe the MEDI of small argon clusters [23]. The Ar_n inner barriers decrease with cluster size. In the Ar_{13} cluster they vanish between adjacent atoms, in contrast to smaller clusters. On the basis of this analysis we suggest that Ar_{13} and larger Ar clusters will demonstrate MEDI.

In the Xe_6 clusters there are inner barriers but they are low and their tunneling parameter T is considerably lower than the parameter T of small argon clusters, in the range of $T \approx 3.5-5.3$ for $q<6$. Such barriers do not prevent MEDI of the Xe_6 clusters in strong laser fields which depress the inner barriers. The MEDI of the xenon clusters has been experimentally detected [25].

In $I^{q+}(Ar^{(q-1)+})_{n-1}$ clusters (Table III) the inner barriers $U_b^{(i)}$ are considerably lower than in the pure argon and xenon clusters, due to lower atomic IP of the iodine ion. As in the pure argon clusters, the $U_b^{(i)}$ values of $I^{q+}(Ar^{(q-1)+})_{n-1}$ decrease with the cluster size. The inner barriers are present ($U_b^{(i)}>0$) in the diatomic $I^{(q+1)+}Ar^{q+}$ (Table II) and in the $I^{q+}(Ar^{(q-1)+})_3$ cluster, but in larger clusters, $I^{q+}(Ar^{(q-1)+})_4$ and $I^{q+}(Ar^{(q-1)+})_5$, they mostly vanish ($U_b^{(i)}<0$). The values $U_b^{(i)}$ are particularly low for nonadjacent pairs of these clusters. Thus, in the $I^{q+}(Ar^{(q-1)+})_5$ cluster the nonadjacent pairs (interionic distance $R=5.72$ Å) do not have any barrier ($U_b^{(i)}<0$) in the wide interval of charges $1<q<6$. The absence of inner barriers in relatively large $I^{q+}(Ar^{(q-1)+})_{n-1}$ ($n>4$) clusters raises the distinct possibility that these clusters are subjected to MEDI [29], thus explaining the high energy of product atomic ions in the experiments of Castleman *et al.* on these systems [23].

Due to the suppression of inner barriers in a charged cluster individual ions lose a few electrons, which become delocalized inside the cluster. Such a process can be called an inner ionization. The energy of the delocalized electrons is enhanced by the outer field in an effective way as was demonstrated recently by the trajectory calculation of electron dynamics in multicharged clusters [44]. The inner ionization is realized, however, only in already charged clusters, which raises the problem of the initial ionization or ignitation process [32,44].

IV. DYNAMIC ENHANCEMENT OF THE ELECTRON ENERGY

As stated in Sec. II the quasiresonance conditions for electron energy enhancement can be satisfied in the presence of an inner barrier that increases the time for the electron motion between ions. In the case of a frozen nuclear geometry the energy enhancement process was supposed to be connected with tunneling [39]. We will now try to find a mechanism of electron energy enhancement that will be of pure classical origin. Let us consider the situation where in the absence of an outer field there is an inner barrier that prevents the classical electron motion between ions ($U_b^{(i)}>0$), so that the electron is located in one of the potential wells, e.g., the left one (Fig. 1). In the presence of an outer field whose frequency is considerably lower than the characteristic frequency of electron motion ($\nu_F \ll \nu_e$), the electron energy varies roughly in the range of $\Delta E = \pm eF_0 l$, where l is the path of electron motion inside the ionic well. Taking a realistic value of $eF_0 = 2.74$ eV/Å ($S=10^{14}$ W/cm^2) and $l=3$ Å one estimates $|\Delta E| \approx 8$ eV. When the force eF is directed to the right the electron can gain energy ΔE larger than $U_b^{(i)}$, overcome the inner barrier, and transfer to the rightsided ion. After reaching the turning point the electron goes back to the left, i.e., against the force eF, losing some portion of its energy. If the inner barrier is fixed (a frozen nuclear geometry) the electron comes back to the left potential well without any significant gain or loss of energy. The situation is quite different when the inner barrier is not fixed but is rising in time. In this case the electron can be trapped in the right well by the rising inner barrier. Only when the field direction is reversed, the electron can again overcome the inner barrier and go to the left well, once more increasing its energy. Such a jump over the rising barrier can be repeated several times, causing an important enhancement of the electron energy. This sequence of events is repeated until the electron energy becomes higher than the electrostatic barrier and the electron leaves the system. This process of the ionization of a multicharged system with the rising inner barrier will be referred to as dynamic CREI.

The time-dependent inner potential is realized in the multicharged molecules and clusters due to the Coulomb explosion, which leads to the increase of the interionic distances R [see Eqs. (3), (19), and (20)]. The increase of the interionic distances in the course of the Coulomb explosion will induce ionization by a purely classical mechanism of the dynamic CREI. In order to study this new mechanism we performed trajectory calculations of electrons in multicharged systems irradiated by a laser field. The calculations were performed in a one-dimensional and one-electron approximation, as in the works of Seideman *et al.* [39] and Chelkowski and Bandrauk [38]. The one-electron approach is based on the assumption of a sequential mechanism of the multielectron ionization, which ignores the possibility of a collective removal of more than one electron at the same time. For the electron-ions potential we used a one-dimensional Coulomb potential [38,39] along the x coordinate

$$V(x) = -B \sum_i \frac{q_i}{R_i}, \tag{22}$$

where q_i are the ion charges and R_i are the electron-ion distances. Considering the electron motion between two ions ($i=1,2$, for example) we shift these atoms from the trajectory coordinate x by some distance b (a smoothing parameter) [38,39]. We used a relatively low value of $b=0.3$ Å, whereas in Refs. [38] and [39] the value of about 1 Å was taken. However, we found that the electron motion is not sensitive to the smoothing parameter value. In order to take into account, at least indirectly, the real potential in the vi-

cinity of nuclei and the strong quantum character of the electron motion there, the initial electron energy in the absence of an outer field is determined by the experimental IP [see Eqs. (4) and (13)]. The equation of motion is

$$\frac{d^2x}{dt^2}=C\left[-B\sum\ \frac{x-x_i}{R_i^3}+eF_0\cos(2\pi\nu_F+\varphi_0)\right];$$

$$C=17.604\ \text{Å}\ \text{fs}^{-2}\,\text{eV}^{-1}, \tag{23}$$

where x and R are in Å, t is in fs, and eF_0 is in eV/Å. The initial conditions are determined by the initial electron location x_0, velocity v_0, and phase φ_0. The initial coordinates x_0 and velocities v_0 of the electron trajectories are chosen by considering the electron motion at the initial nuclear geometry in the absence of the outer field and dividing the motion period on equidistant time steps. The initial phases φ_0 of the outer field are equidistantly separated. Our classical treatment of the ionization process is restricted here to one-color excitation. It would be of interest to extend our treatment to consider the case of two-color excitation in order to study the high-energy enhancement process proposed recently by Bandrauk *et al.* [45].

Before treating the dynamic CREI we performed classical trajectory calculations for the frozen geometry Cl_2 ions in order to compare the classical results with the quantum results of Refs. [38] and [39]. The classical calculations were performed for a moderately strong laser intensity of $S=10^{14}$ W/cm^2 and a frequency $\nu_F=0.38$ fs^{-1}. In these classical calculations we did not find any $Cl^{2+}Cl^{3+}\rightarrow Cl^{3+}Cl^{3+}$ $(q=3)$ ionization in the wide interval of interionic distances and estimated the upper limit for the ionization rate as 5×10^{-5} fs^{-1}. Since the quantum calculation provides a much larger ionization rate of 2.5×10^{-3} fs^{-1} at maximum [38], in accord with the estimates of Table I, we conclude that for $q=3$, and surely for $q>3$, the CREI is of pure quantum origin. The results are quite different for $Cl^{1+}Cl^{2+}\rightarrow Cl^{2+}Cl^{2+}$ $(q=2)$ ionization. In this case the classical calculation provides ionization rates that are close to the quantum results of Ref. [39]. For example, both our classical treatment for $S=10^{14}$ W/cm^2 and the quantum calculation of Ref. [39] for $S=0.9\times10^{14}$ W/cm^2 provide maximal ionization rates of about 3%. It follows that for small q, when the electrostatic barrier is relatively low, the ionization is mostly of classical origin and it is not connected with the process of the quasiresonance energy enhancement.

In systems with a fixed ion geometry the ionization process is realized provided that the electron energy is positive after the end of the laser pulse. Treating the dynamic CREI of a Coulomb exploding system we cannot be restricted by this simple criterion of ionization since the electron energy is steadily increasing in the absence of an outer field, i.e., after the end of the laser pulse. At final (infinite) interionic distances this electron may be either weakly bound to one of the ions $(E<0)$ or in the unbound (ionization) state $(E>0)$. The weakly bound electron is expected to occupy a high Rydberg state. The presence of Rydberg excited ions (or neutral atoms) among the products of the Coulomb explosion affects the energetics of the Coulomb explosion as these ions capture (or recapture) electrons at large interionic distances. Accordingly, their kinetic energy is determined not by the final charge but by some higher charge that these ions had during the early stage of the Coulomb explosion. Since it is difficult to specify the final states of electrons that are found outside the ionic system and that have a negative (mostly small) energy at the end of the laser pulse, we will put them in one group that will be denoted by in-ex (ionization or excitation).

TABLE IV. Dynamic CREI of the $I^{4+}(Ar^{4+})_5\rightarrow I^{5+}(Ar^{4+})_5$ ionization process. The dependence of ionization P_{in} and ionization-excitation $P_{\text{in-ex}}$ probabilities (in %), the average time of electron removal t_{in} (in fs), and the average interionic distance of electron removal R_{in} (in Å) on the dissociation dynamics parameter q' (see text) and on the light frequency ν_F (in fs^{-1}) are presented. The initial (equilibrium) I-Ar distance is $R_e=5.72$ Å. The light intensity is $S=10^{14}$ W/cm^2.

q'	ν_F	P_{in}	$P_{\text{in-ex}}$	t_{in}	R_{in}
1	0.5	52.5	3.3	84.9	8.6
2	0.5	53.3	3.3	45.1	8.9
4	0.5	42.5	5.8	24.2	9.2
4	0.25	56.5	0.9	31.4	10.8
4	1.0	38.0	26.8	19.4	8.2

In the trajectory calculations of the dynamic CREI we use the equilibrium nuclear neutral state configuration as the starting point of the Coulomb explosion. The dynamics of ion expansion is determined by the ion charges, and the dynamics of Coulomb explosion was simulated using our previous formalism [29]. Ignoring the increase of the ionic charges in the course of the Coulomb explosion, we assume the expansion dynamics of fixed ion charges to be q'. According to our calculation of diatomic Cl_2, the ionization probability dependence on q', and consequently on the ion expansion velocity, is within a numerical factor of 2. For example, in the case of the ionization process

$$Cl^{2+}Cl^{3+}\rightarrow Cl^{3+}Cl^{3+} \tag{24}$$

at $S=10^{14}$ W/cm^2, the ionic charges of $q'=3$ provide the ionization probability of 13.3%, whereas in the case of $q'=1$ the corresponding number is 24.2%. In the case of the IAr_5 cluster the q' effect is much weaker (Table IV).

The dynamic ionization probability P_{in} dependence on the light power S is presented in Fig. 2 for the ionization process (24) and for the cluster expansion parameter $q'=1$. In Fig. 2 we also present results for the ionization probability in the static geometry estimated using the time-dependent ionization probabilities of Chelkowski and Bandrauk [38] together with the passage time through the region of high ionization efficiency inferred from their simulation. According to the results presented in Fig. 2 the dynamic CREI is considerably more efficient than the frozen geometry CREI. The ionization probability increases with increasing the laser intensity in the studied range $S=2\times10^{13}$–10^{15} W/cm^2. A most striking result of the dynamic CREI calculation is a moderately slow decrease of the ionization probability with the decrease of the laser intensity. When the intensity is relatively low, e.g., $S=2\times10^{13}$ W/cm^2 $(eF_0=1.228$ eV/Å), the ionization probability is still not negligibly small, being about 0.3%. When the laser field intensity increases to

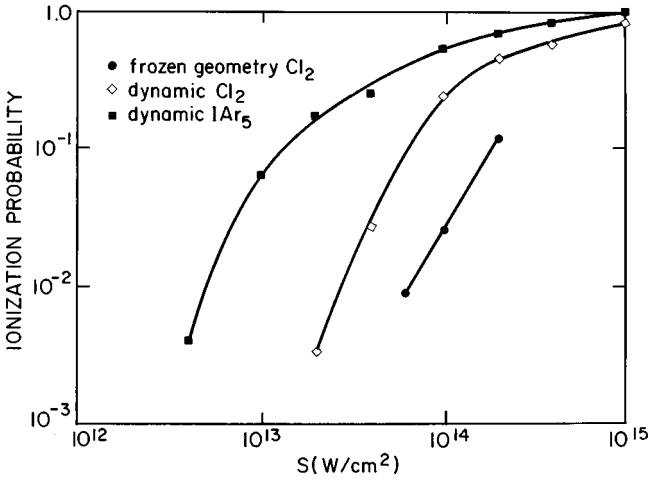

FIG. 2. The simulated dynamic CREI data for Cl_2 and IAr_5 (this work) and the frozen geometry CREI data for Cl_2 (inferred from Ref. [38], see text), showing the ionization probability P_{in} dependence on light intensity S (in W/cm^2) for $Cl^{2+}Cl^{3+} \rightarrow Cl^{3+}Cl^{3+}$ ($q'=1$, $\nu_F=0.38$ fs^{-1}) and for $I^{4+}(Ar^{4+})_5 \rightarrow I^{5+}(Ar^{4+})_5$ ($q'=2$, $\nu_F=0.5$ fs^{-1}) ionization processes.

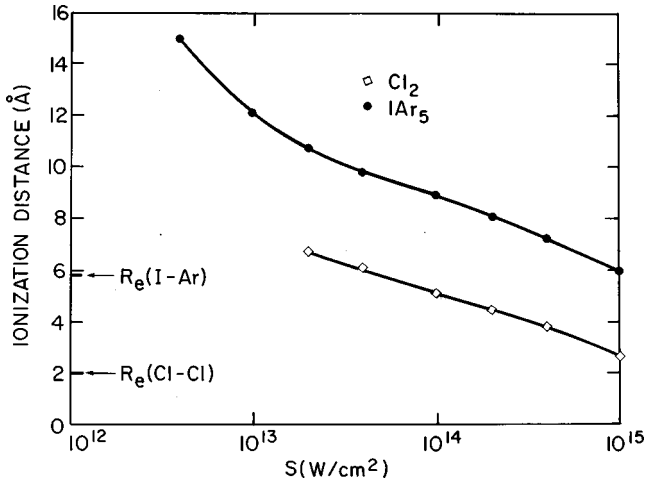

FIG. 3. The simulated dynamic CREI ionization distance R_{in} dependence on the light intensity S (in W/cm^2). For details, see Fig. 2.

$S=6\times10^{13}$ W/cm^2 the ionization probability becomes $P_{in}\sim10\%$, being by one order of magnitude higher than the frozen geometry value. The moderately strong intensity of 10^{14} W/cm^2 ($eF_0=2.744$ eV/Å) provides an ionization probability of $P_{in}\approx24\%$. In the very strong field of 10^{15} W/cm^2 only a small part of the molecules, about 20%, remains unionized. The probability of the in-ex process in the Cl_2 molecule was found to be several times smaller than P_{in}.

When the ionization probability P_{in} is high some 25%–40% of the ions lose the electrons at the very beginning of the laser pulse at $R\sim R_e$ (vertical ionization) by a direct outer field force. The rest of the removed electrons undergo a short process of quasiresonance energy enhancement and abandon the molecules at $R>R_e$, mostly at interionic distances $R_{in}\approx3.0$–3.5 Å (nonvertical ionization). When P_{in} is not high the distance of electron removal R_{in} is scattered (by about 20%) around its average value. Such behavior indicates the presence of some relatively narrow R intervals where the electron energy enhancement is efficient. The occurrence of a narrow R domain for ionization is in accordance with the experimental findings [46]. The dependence of the average R_{in} on the light intensity S for the ionization process (24) is presented in Fig. 3. The R_{in} distance decreases monotonously with increasing S. At relatively weak intensities R_{in} is more than three times larger than the equilibrium distance R_e. In the strong field of $S=10^{15}$ W/cm^2, R_{in} exceeds R_e by only 30%.

The temporal dynamics of the ionization process is reflected in the ionization times t_{in}. The ionization efficiency is practically independent on the pulse length τ, if τ noticeably exceeds the average ionization time t_{in}. The average t_{in} dependence on S is presented in Fig. 4. The ionization time t_{in} decreases monotonously with S, like the ionization distance R_{in}. In the strong field of $S=10^{15}$ W/cm^2 the ionization process takes 23 fs or about 9 of the electromagnetic field oscillations. In the interval 2×10^{13}–4×10^{14} W/cm^2 t_{in} depends nearly linearly on log S.

The ionization probability dependence on the atomic charge q for the ionization process $Cl^{(q-1)+}Cl^{q+} \rightarrow Cl^{q+}Cl^{q+}$ ($q'=1$, $S=10^{14}$ W/cm^2) is presented in Fig. 5. The ionization probability steeply decreases with q for $q>3$ and becomes less than 0.1% for $q>6$, when the $3s$ electrons are removed.

The dynamic CREI mechanism in vdW clusters has been studied for the case of the IAr_5 cluster (Figs. 2–5). In these calculations the electron trajectory is located at the distance of 0.3 Å (the smoothing parameter b) from the IAr line of a nonadjacent pair. The initial (equilibrium) IAr distance is $R_e=5.72$ Å. The ionization probability P_{in} dependence on S is shown in Fig. 2 for the ionization process $I^{4+}(Ar^{4+})_5 \rightarrow I^{5+}(Ar^{4+})_5$ ($q'=2$, $\nu_F=0.5$ fs^{-1}). The ionization efficiency in the vdW cluster IAr_5 is much higher than in the valence Cl_2 molecule. Thus, in the relatively low field intensity of 10^{13} W/cm^2 the ionization probability in the cluster is about 6% whereas in Cl_2 with lower charges it is smaller than 0.1%. At moderate and strong intensities of $S\geqslant2\times10^{13}$ W/cm^2 the probability $R_{in\text{-}ex}$ is smaller than P_{in} but at relatively low intensities of $S=4\times10^{12}$–10^{13} W/cm^2 $P_{in\text{-}ex}$ becomes larger, mostly about twice, than P_{in}, which

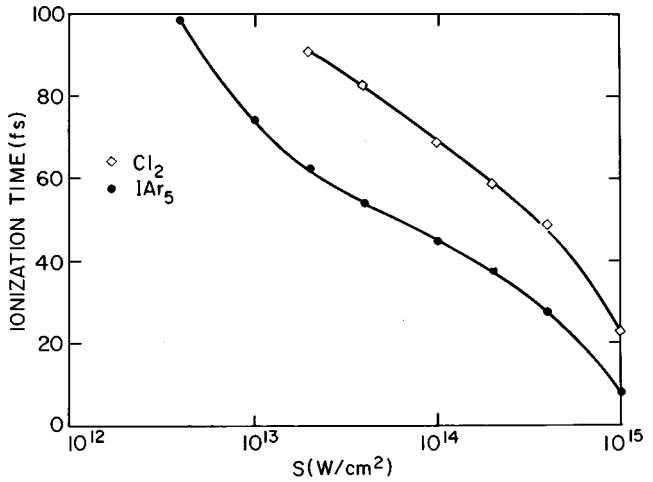

FIG. 4. The simulated dynamic CREI ionization time t_{in} dependence on the light intensity S (in W/cm^2). For details, see Fig. 2.

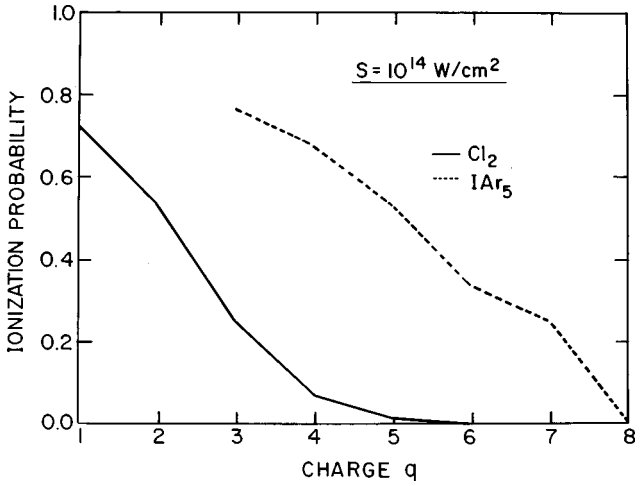

FIG. 5. The simulated dynamic CREI ionization probability P_{in} dependence on the ionic charge q for $Cl^{(q-1)+}Cl^{q+} \rightarrow Cl^{q+}Cl^{q+}$ ($q'=1$, $\nu_F=0.38\ \text{fs}^{-1}$) and for $I^{(q-1)+}(Ar^{(q-1)+})_5 \rightarrow I^{q+}(Ar^{(q-1)+})_5$ ($q'=2$, $\nu_F=0.5\ \text{fs}^{-1}$) ionization processes. The light intensity is $S=10^{14}$ W/cm^2.

implies that a large number of Rydberg excited ions may be detected.

In a very strong field of 10^{15} W/cm^2 most of the removed electrons, about 60%, abandon the system at $R \sim R_e$, which supports the assumption previously accepted by us of a vertical ionization in these clusters [29]. The average ionization distance in so strong a field is $R_{\text{in}}=6.1$ Å, which is only 0.3 Å larger than the equilibrium distance R_e (Fig. 3). In weaker fields the distances R_{in} of electron removal from the vdW clusters are scattered in a roughly symmetrical way around an average value $R_{\text{in}} > R_e$ (nonvertical ionization) although with a bigger dispersion than in Cl_2. The ionization times t_{in} roughly fall into the same time range as in Cl_2 (Fig. 4).

The effect of the ion expansion velocity (determined by the charge q') on the ionization probability is very weak (Table IV). We also checked the CREI efficiency dependence on the light frequency ν_F. The ionization probability P_{in} decreases significantly with ν_F but at the same time the $P_{\text{in-ex}}$ probability increases, so that the sum $P_{\text{in}}+P_{\text{in-ex}}$ weakly depends on ν_F. The ionization probability P_{in} dependence on the iodine charge q is presented in Fig. 5 for $S=10^{14}$ W/cm^2. The interesting finding of our calculation is the high efficiency of the formation of highly charged ions with $q=7$. The ionization probability drops, however, to zero (or, more exactly, to $P_{\text{in}}<0.1\%$) at $q=8$ ($4d$-electron ionization). The $4d$-electron ionization is also absent in a stronger field of $S=10^{15}$ W/cm^2.

The field-induced electron energy enhancement resulting from the increase of inner potential barriers may be of importance not only in the MEDI process. Such energy enhancement may be realized in any system where the electron potential has the shape of potential wells separated by potential barriers that rise in time.

V. CONCLUSIONS

From the analysis of multielectron dissociative ionization of diatomics and clusters the following conclusions emerge

(1) Features of the charge resonance enhanced ionization (CREI) mechanism: The CREI mechanism [37,38] cannot be realized in a multicharged system if at equilibrium (neutral state) geometry there are large inner potential barriers that prevent electron motion between ions. The CREI mechanism can only be effective when the system initially has some ionic pairs without any inner barrier or with relatively transparent inner barriers. According to this criterion the CREI mechanism is expected to be efficient in valence diatomics, e.g., Cl_2 and I_2, and vdW heteroclusters, e.g., IAr_n, but not in most homonuclear rare-gas diatomics and in small neat rare-gas clusters.

(2) Interionic distances for CREI: In those systems where an effective CREI mechanism prevails, such as for valence molecules Cl_2 and I_2 and the IAr_n cluster, multielectron ionization takes place at distances R, which are larger than the equilibrium distance R_e (nonvertical ionization) and lie in the interval $R_b<R<R_T$. In this interval the inner barrier exists ($R>R_b>R_e$) and this barrier is transparent ($R<R_T$). At the beginning of laser irradiation, when the system is in the equilibrium geometry, the electrostatic barrier suppression mechanism [47] is responsible for the preliminary ionization of the system atoms, which, most probably, become singly ionized. The preliminary ionization is followed by the Coulomb expansion up to the interionic distance R_b, where the system begins to lose more electrons due to the CREI mechanism.

(3) Effect of very strong laser fields: In these fields, mostly $S \geqslant 10^{15}$ W/cm^2, the barrier suppression mechanism may be responsible not only for preliminary but also for multielectron vertical ionization.

(4) Classical and quantum effects on CREI: The simulation of electron motion for a frozen molecule geometry shows that the ionization process $Cl^{(q-1)+}Cl^{q+} \rightarrow Cl^{q+}Cl^{q+}$ in the field of 10^{14} W/cm^2 is of purely quantum (tunneling effect) origin for $q>3$, whereas for $q \leqslant 2$ the ionization is of mostly classical origin.

(5) Dynamic CREI: Since, due to the Coulomb explosion, multicharged molecules and clusters are spatially expanding systems, their inner barriers rise in time. It has been shown that in the presence of a strong laser field the electron energy can be increasing at, roughly, the same rate as the level of the barrier top. Such a dynamic mechanism of the electron energy enhancement is classically feasible. The simulation study of the electron motion in the multicharged Cl_2 and IAr_5 demonstrates high efficiency of the multielectron ionization by this mechanism, which is considerably more efficient than the static CREI. The ionization probabilities provided by the dynamic mechanism increase with the field power increase in the range $S=10^{13}-10^{15}$ W/cm^2. The field power dependence of the dynamic mechanism is much weaker than the frozen nuclear geometry calculations of Seideman, Ivanov, Corkum [39] and Chelkowski and Bandrauk [38].

(6) Dynamic quasiresonance energy enhancement: The laser-field-induced energy enhancement of any charged particle may be realized in any system where the particle can move between two potential wells separated by a potential barrier that rises during the laser pulse irradiation.

ACKNOWLEDGMENT

This research was supported by the Binational German-Israeli James Franck program on Laser Matter Interaction.

[1] A. J. Stace, in *The Chemical Physics of Atomic and Molecular Clusters*, edited by G. Scoles (Elsevier, Amsterdam, 1990).
[2] F. A. Gianturco and M. P. de Lara-Castells, Chem. Phys. **208**, 25 (1996).
[3] R. Casero and J. M. Soler, J. Chem. Phys. **95**, 2927 (1991).
[4] J. G. Gay and B. J. Berne, Phys. Rev. Lett. **49**, 194 (1982).
[5] E. Ruhl, C. Schmale, H. C. Schmelz, and H. Baumgartel, Chem. Phys. Lett. **191**, 430 (1992).
[6] I. Last and T. F. George, Chem. Phys. Lett. **216**, 599 (1993).
[7] K. Sattler, J. Muhlbach, O. Echt, P. Pfau, and E. Recknagel, Phys. Rev. Lett. **47**, 160 (1981).
[8] C. Bréchignac, Ph. Cahuzac, F. Carlier, and M. de Frutos, Phys. Rev. B **49**, 2825 (1994).
[9] C. Bréchignac, Ph. Cahuzac, F. Carlier, M. de Frutos, J. Leygnier, and J. Ph. Roux, J. Chem. Phys. **102**, 763 (1995).
[10] M. Lezius and T. D. Märk, Chem. Phys. Lett. **155**, 496 (1989).
[11] A. J. Stace, P. G. Lethbridge, and J. E. Upham, J. Phys. Chem. **93**, 333 (1989).
[12] A. Goldberg, I. Last, and T. F. George, J. Chem. Phys. **100**, 8277 (1994).
[13] D. Kreisle, O. Echt, M. Knapp, E. Recknagel, K. Leiter, T. D. Märk, J. J. Saenz, and J. M. Soler, Phys. Rev. Lett. **56**, 1551 (1986).
[14] M. Lezius, P. Scheier, A. Stamatovic, and T. Märk, J. Chem. Phys. **91**, 3240 (1989).
[15] P. Scheier and T. D. Märk, Phys. Rev. Lett. **73**, 54 (1994).
[16] A. l'Huiller, L. A. Lompre, G. Mainfray, and C. Manus, Phys. Rev. A **27**, 2503 (1983).
[17] T. S. Luk, U. Johann, H. Egger, H. Pummer, and C. K. Rhodes, Phys. Rev. A **32**, 214 (1985).
[18] K. Boyer, T. S. Luk, J. C. Solem, and C. K. Rhodes, Phys. Rev. A **39**, 1186 (1989).
[19] C. Cornaggia, J. Lavancier, D. Normand, J. Morellec, and H. X. Liu, Phys. Rev. A **42**, 5464 (1990).
[20] J. Lavancier, D. Normand, C. Cornaggia, J. Morellec, and H. X. Liu, Phys. Rev. A **43**, 1461 (1991).
[21] K. Codling, L. J. Frasinski, P. Hatherly, and J. R. M. Barr, J. Phys. B **20**, L525 (1987).
[22] D. P. Armstrong, D. A. Harkins, R. N. Compton, and D. Ding, J. Chem. Phys. **100**, 28 (1994).
[23] J. Purnell, E. M. Snyder, S. Wei, and A. W. Castleman, Jr., Chem. Phys. Lett. **229**, 333 (1994).
[24] E. M. Snyder, S. Wei, J. Purnell, S. A. Buzza, A. W. Castleman, Jr., Chem. Phys. Lett. **248**, 1 (1996).
[25] E. M. Snyder, S. A. Buzza, and A. W. Castleman, Jr., Phys. Rev. Lett. **77**, 3347 (1996).
[26] T. Ditmire, T. Donnelly, A. M. Rubenchik, R. W. Falcone, and M. D. Perry, Phys. Rev. A **53**, 3379 (1996).
[27] T. Ditmire, J. W. G. Tisch, E. Springate, M. B. Mason, N. Hay, J. P. Marangos, and M. H. R. Hutchinson, Phys. Rev. Lett. **78**, 2732 (1997).
[28] T. Ditmire, J. W. G. Tisch, E. Springate, M. B. Mason, N. Hay, R. A. Smith, J. Marangos, and M. H. R. Hutchinson, Nature (London) **386**, 54 (1997).
[29] I. Last, I. Schek, and J. Jortner, J. Chem. Phys. **107**, 6685 (1997).
[30] L. V. Keldysh, Sov. Phys. JETP **20**, 1307 (1965).
[31] H. A. Bethe and E. E. Salpeter, *Quantum Mechanics of One- and Two-Electron Atoms* (Springer-Verlag, Berlin, 1957).
[32] C. Rose-Petruck, K. J. Schafer, and C. P. J. Barty, Proc. SPIE Int. Soc. Opt. Eng. **2523**, 272 (1995).
[33] M. Schmidt, D. Normand, and C. Cornaggia, Phys. Rev. A **50**, 5037 (1994).
[34] M. Yuan and T. F. George, J. Chem. Phys. **68**, 3040 (1978).
[35] P. Schwender, F. Seul, and R. Schinke, Chem. Phys. **217**, 233 (1997).
[36] T. Zuo, S. Chelkowski, and A. D. Bandrauk, Phys. Rev. A **48**, 3837 (1993).
[37] T. Zuo and A. D. Bandrauk, Phys. Rev. A **52**, R2511 (1995).
[38] S. Chelkowski and A. D. Bandrauk, J. Phys. B **28**, L723 (1995).
[39] T. Seideman, M. Yu. Ivanov, and P. B. Corkum, Phys. Rev. Lett. **75**, 2819 (1995).
[40] S. Chelkowski, A. Conjusteau, T. Zuo, and A. D. Bandrauk, Phys. Rev. A **54**, 3235 (1996).
[41] K. Colding, L. J. Frasinski, and P. A. Hatherly, J. Phys. B **22**, L321 (1989).
[42] L. I. Schiff, *Quantum Mechanics* (McGraw-Hill, New York, 1955).
[43] R. D. Cowan, *The Theory of Atomic Structure and Spectra* (University of California Press, Berkeley, 1981).
[44] C. Rose-Petruck, K. J. Schafer, K. R. Wilson, and C. P. J. Barty, Phys. Rev. A **55**, 1182 (1997).
[45] A. D. Bandrauk, S. Chelkowski, H. Yu, and E. Constant, Phys. Rev. A **56**, R2537 (1997).
[46] C. Cornaggia, J. Lavancier, D. Normand, J. Morellec, P. Agostiny, J. P. Chambaret, and A. Antonetti, Phys. Rev. A **44**, 4499 (1991).
[47] S. Augst, D. Strickland, D. Meyerhofer, S. L. Chin, and J. H. Eberly, Phys. Rev. Lett. **63**, 2212 (1989).